(Proceedings ModelCARE2011 held at Leipzig, Germany, in September 2011) (IAHS Publ. 355, 2012).

A GIS-linked unit response function approach to stochastic groundwater nonpoint source pollution modelling

GEORGE KOURAKOS, FRANK KLEIN & THOMAS HARTER
Department of Land Air and Water Resources, University of California, Davis, California, USA
giorgk@gmail.com

Abstract A 3-D groundwater flow and transport modelling algorithm specifically designed for nonpoint source transport modelling is applied to a large groundwater sub-basin of the Central Valley, California, USA, to simulate and predict spatio-temporally distributed nitrate contamination over a century-long period. A simplistic domain decomposition method is proposed to simulate the velocity field (flow) at the decameter scale across a 2000 km^2 domain. A streamline transport model is used to simulate the fate of contaminants and to link a large number (>10^3) of discrete discharge surfaces (production wells) with an even larger number (~10^4) of individual contaminant sources via unit response functions. Based on the historic and projected, spatio-temporally variable nitrate recharge history, nitrate output at wells is predicted via convolution of loading functions with unit response functions and integration across individual discharge surfaces. The results show that 45% of wells in this agricultural groundwater basin exceed the drinking limit in 2011, with an increase to 58% in 2050, despite an assumed reduction of nitrate recharge rates after 2011.

Key words nonpoint source modelling; streamline transport model; domain decomposition method; unit response functions; nitrate contamination; Central Valley, California

INTRODUCTION

Groundwater degradation due to pollution from nonpoint sources (NPS) is an emerging challenge to global water security and health (WWAP, 2009). Agriculture is the most dominant polluter, primarily through emissions of nitrogen and salt but also pesticides and other farm-chemicals (Bower, 2000; Watanabe *et al*., 2010). Sound policy requires thorough scientific understanding of nonpoint sources and how they work, and of the linkage between nonpoint sources and groundwater discharges to users or affected ecosystems (domestic wells, irrigation wells, urban/municipal wells, springs, discharges to stream reaches). Significant scientific effort has been dedicated to understand, manage and monitor potential sources, to understand the dynamics of NPS pollutants and to assess the consequences, and various modelling approaches have been developed such as statistical models, index methods, and process-based models.

At the basin scale, statistical models (Nolan *et al*., 2002; Sorichetta *et al*., 2011) and index methods (Civita & De Maio, 2004; Javadi *et al*., 2011) have been used to provide decision-makers with qualitative estimates of the effect of NPS pollution across a groundwater basin. However, nonpoint sources exhibit significant variability across source types (agricultural crops, septic leach field, ponding basins/lagoons) and among similar sources managed by different landowners and subject to variable land uses (e.g. varying crops). Nonpoint source loading is also highly variable in time. To assess nitrate and other NPS pollution in domestic and public supply wells, spatial variability must be resolved to the scale of individual wells and their source area or finer. For some NPS pollutants, such as nitrate and salinity, which typically vary over a relatively narrow range near regulatory limits (± one order of magnitude), temporal variations of source loading at the annual and inter-annual scale drive subsequent well pollutant levels, while shorter-term and very small-scale variations in the pollutant signal are absorbed by the mixing that occurs in typical production well screens. Proper resolution of physical transport processes in groundwater requires high resolution computer models and prohibits the application of high resolution process models to large groundwater basins (10^3 km^2 to 10^5 km^2). Process-based model applications have been limited to site-specific studies of pollution, primarily point source pollution, particularly if aquifer heterogeneity is also considered.

We recently developed a highly efficient process-based groundwater NonPoint Source Assessment Toolbox (NPSAT) (Kourakos *et al*., 2012) that preserves key process characteristics

of groundwater transport from nonpoint sources, while providing an efficient flow and transport modelling approach. In this paper, we develop a domain decomposition method to integrate into NPSAT and demonstrate the applicability of the NPSAT approach to large groundwater basins with a wide range of small-scale heterogeneous nonpoint sources, well locations, and well source areas distributed across the entire basin. Process-based regional modelling is achieved by introducing an automated two-step domain decomposition method where the domain is first simulated using a coarse resolution and is then divided into several overlapping sub-domains for either sequential or parallel high resolution simulation of flow and transport. Boundary conditions for the sub-domains are interpolated from the coarse grid solution, while a weighted average scheme is used to smooth the velocity field across sub-domain boundaries.

The new domain decomposition method used within NPSAT is applied to a 2000 km^2 agricultural groundwater basin in the Central Valley of California. Using a spatio-temporally heterogeneous nitrate loading pattern as the external forcing, we simulate nitrate occurrence in production wells from 1945 to 2050.

NONPOINT SOURCE ASSESSMENT TOOLBOX (NPSAT)

The NPSAT (Kourakos *et al*., 2012) is a flow and transport model for simulating the fate of contaminants in groundwater aquifers, and is intended for applications in regional land-use and groundwater quality management and decision making. The details of the computational method employed in NPSAT are presented by Kourakos *et al*. (2012). Briefly, NPSAT involves two phases (i) a NPS unit response function (URF) construction phase to compute URFs between NPSs and individual wells based on physical solutions of the 3-D flow and quasi-3-D transport equations. URFs are stored into a GIS platform, (ii) in the forward phase, URFs are convoluted with spatio-temporally variable NPS loading functions to predict detailed long-term pollutant breakthrough curves at production wells or stream reaches.

To deal with the demanding computational burden associated with the high resolution simulations necessary to generate physically-based URFs, we propose a two-step simplistic domain decomposition method. Initially the aquifer is treated as a single domain Ω and simulated using a coarse discretization, resulting in a coarse hydraulic head field h^c. In a second step, the domain Ω is divided into N sub-domains $\Omega_1, \Omega_2, \ldots \Omega_N$, which are resolved at very fine resolution. In this application we choose to divide the domain into orthogonal sub-domains, but the same method can be extended to any arbitrary sub-domain shape. We define the boundaries $\partial\Omega$ of domain Ω as external, and the artificial boundaries Γ_n as internal. Note that $\partial\Omega_n$ (i.e. the boundary of sub-domain n) consists either of part of $\partial\Omega$ and Γ_n or exclusively of internal boundaries Γ_n. To assign boundary conditions to internal boundaries Γ_n we use an interpolation method $I_{\Omega\to\Gamma n}$ where the unknown boundary conditions Γ_n are interpolated from the coarse solution h^c and the fine head field h_n^f for each sub-domain n is calculated independently. At the end of this process, h^f is the union of all individual simulations results $h^f = h_1^f \cup h_2^f \cup \ldots \cup h_N^f$.

However, based on our simulation results already obtained, it was found that the resultant fine head field h^f exhibit discontinuities across the internal boundaries Γ_n. To alleviate this problem, we propose to offset the artificial sub-domains boundaries at a specified distance l_{of} thus producing an overlapping zone of width $2l_{of}$. As shown in Fig. 1(a) the aquifer domain can be of any arbitrary shape, and the simulated area of each sub-domain is defined as the intersection of domain Ω and the extended sub-domain boundary.

Let i be a discrete point, located within the j non-extended sub-domain and also within M extended sub-domains (e.g. in Fig. 1(a), the point i is located within the 2nd non-extended sub-domain and in the 8th extended sub-domain e.g. M = 1). Each sub-domain has a slightly different solution $h_i^j \neq h_i^k \neq h_i^{k+1} \neq \ldots \neq h_i^M$ as a result of the different boundary conditions, where $k \in [1, M]$ are the subdomain IDs. In the case of nonconforming meshes, an interpolated value is

used for the heads $h_i^k, h_i^{k+1}, \ldots, h_i^M$. Subsequently the M + 1 head values can be averaged to obtain the head for point i . However, it has been observed that points closer to the boundaries have a larger head discrepancy from true head values. To counteract this problem, we propose a weighted average scheme, where the weights are taken proportional to the distance from the barycentre of each sub-domain:

$$\overline{h_i} = \frac{1}{\sum_n^M w_i^n} \sum_{j=0}^{M} w_i^n h_i^n; \quad n \in [j, k, k+1, \ldots, M] \tag{1}$$

where h_i^n is the calculated head of point i based on the solution of sub-domain Ω_n and w_i^n is the weight of point i with respect to sub-domain n calculated by the following empirical formula:

$$w_i^n = \min\left\{ W\left({}^{l_x}\!/_2 , l_{of}, \left| x_i - x_c^n \right| \right), W\left({}^{l_y}\!/_2 , l_{of}, \left| y_i - y_c^n \right| \right) \right\} \tag{2}$$

where x_i, y_i are the coordinates of the point i, l_x, l_y are the sub-domain lengths before the offset operator along the x and y directions, respectively, x_c^n, y_c^n are the coordinates of the barycentre of the orthogonal and W is a geometric function defined as:

$$W(l, d, x) = \frac{x - (l + d)}{-2d} \tag{3}$$

It can be seen from equation (2) that input arguments l and d of equation (3) are constants for each sub-domain. Equation (2) returns zero weights for the points that lie on the outer offset edges and weights of ones at the inner offset edges, with weights that vary linearly within the overlapping zone between these two numbers (Fig. 1(c)). The negative weights outside the extended orthogonal are not used and they are ignored. The result of the above formulation is a smooth velocity field across the artificial boundaries.

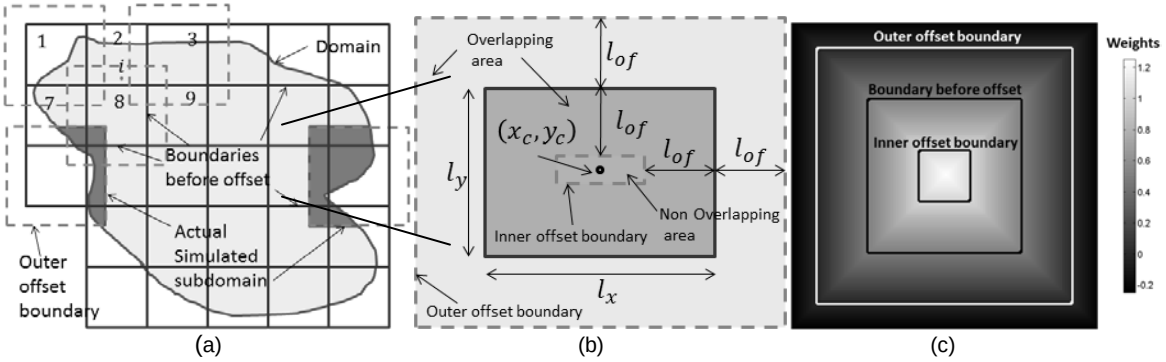

Fig. 1 (a) Decomposition of domain into orthogonal sub-domains. (b) Geometric definition of symbols involved in the domain decomposition method. (c) Weight function.

The velocity field is then used for the transport simulation phase of the NPSAT to obtain a highly efficient, streamline-based quasi-3-D solution of a (user-selected) solute transport equation yielding a pollutant URF (Kourakos *et al*., 2012).

STUDY AREA DESCRIPTION

The study area overlies an extensive alluvial groundwater basin, located in the southwest part of the Central Valley, California (Fig. 2). The study area is part of the Tulare Lake Basin (TLB), which is an intensively farmed agricultural area that relies heavily on groundwater extractions.

Figure 2 illustrates the major land use classes. Each of these land uses can be thought as possible sources of groundwater nitrate contamination through the intensive use of industrial and animal fertilizers. In this basin, groundwater discharge occurs almost exclusively via agricultural, municipal, and domestic production wells distributed laterally and in depth across the highly heterogeneous aquifer system. The TLB aquifer system is typically about 600 m thick, but feathers out in its eastern-most area towards its eastern boundary against the mostly granitic Sierra Nevada mountain range. Regional groundwater flowlines bound the groundwater sub-basin to the north and south, and a no-flow boundary occurs at the valley trough to the west (Ruud *et al*., 2004). Hydraulic conductivity was estimated using pilot point method and varies between 1 m/day to 180 m/day (Ruud *et al*., 2003). Additional details regarding the hydrogeology of the groundwater aquifer, the water budget allocation and stress estimation are given in Ruud *et al*. (2004).

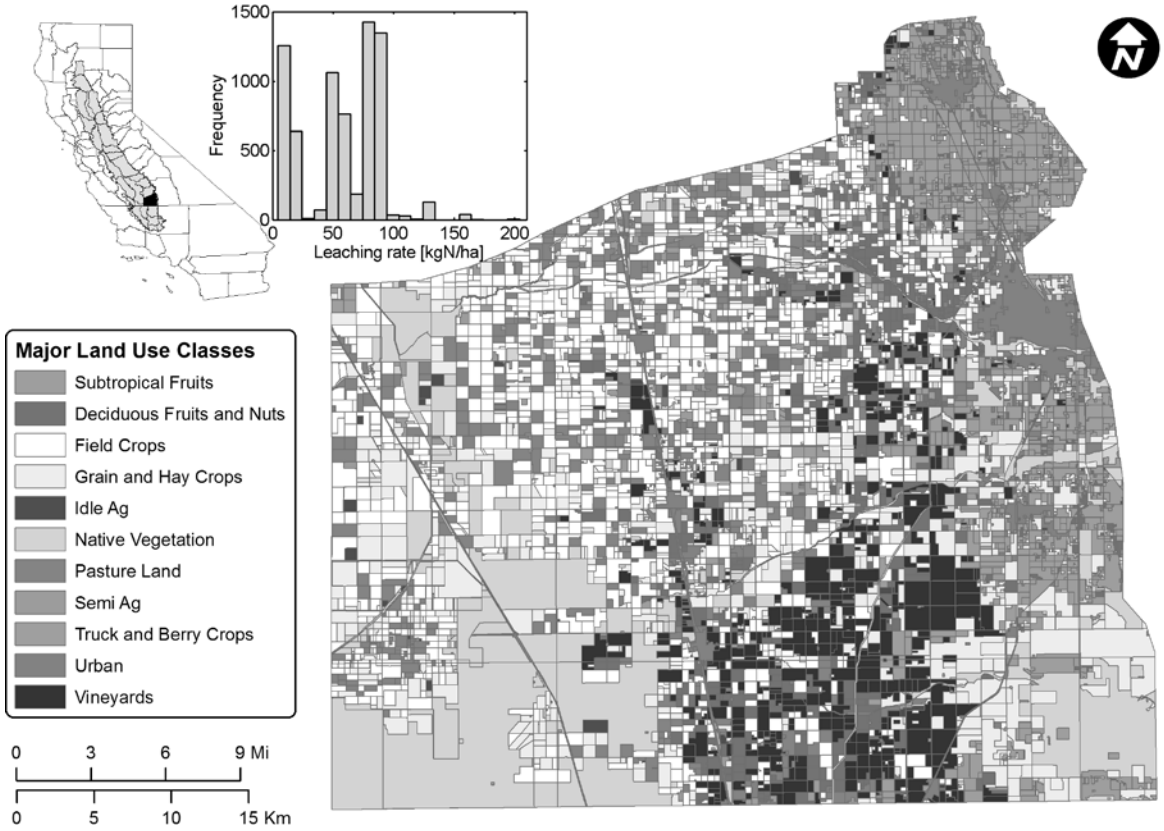

Fig. 2 Study area. The embedded graph shows the histogram of leaching losses into the aquifer.

In this paper we use separate loading functions for each individual crop type. Preliminary estimates of current nitrate leaching rates (mass/area) for each crop were obtained from an ongoing study (http://www.swrcb.ca.gov/water_issues/programs/nitrate_project/). Leaching of nitrate prior to 1945 is considered negligible; leaching rates in 1945 are assumed to be 30% of modern day leaching rates, increasing linearly through 2011. Future nitrate leaching rates are assumed to decrease linearly to 80% of current values by 2050. In total 61 different land uses are identified according to a land survey of 1985 and the histogram (embedded in Fig. 2) shows the frequency of the leaching losses based on the land use map. The total number of land use parcels is 9154 and 23.5% of them are associated with negligible leaching losses (native vegetation, urban areas, etc.). Note that the histogram shows the frequency of leaching losses when only contributing land uses are taken into consideration. In total 37% of land uses leach less than 10 kg N/ha, 18% of land uses is associated with nitrate losses that vary between 10 and 50 kg N/ha, 42% of land uses are associated with N losses that vary between 50 and 100 kg N/ha and 3% exceed 100 kg N/ha.

RESULTS

Domain decomposition

The domain of the study is approximately 2000 km^2 (Fig. 2), while the size of individual land use areas typically varies between 10^{-2} and 2 km^2. To obtain a sufficient resolution that takes into account pollution from very small sources we employed the proposed simplistic domain decomposition method.

First the aquifer is simulated using a finite difference (FD) numerical approximation. The spatial resolution of the FD approximation is 100 m and three layers are used for the vertical discretization. The boundaries of the aquifer are all considered impervious. A known constant head is assigned to a small area of 1 km^2 to obtain a unique solution. The hydraulic head field obtained from the FD approximation (Fig. 3(a)), is used as the coarse solution h^c.

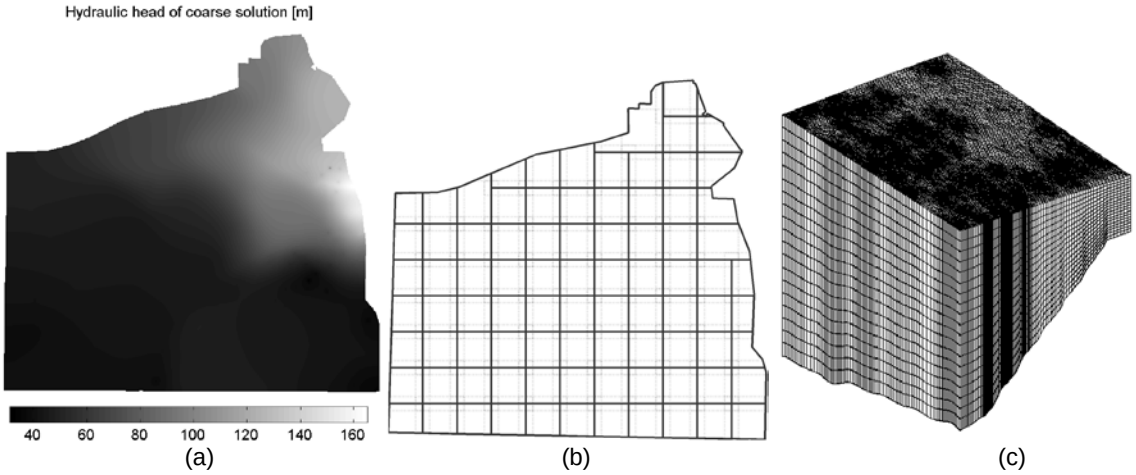

Fig. 3 (a) Coarse solution, (b) the domain divided into 105 overlapping sub-domains, and (c) discretization mesh for the fine solution for a typical subdomain.

Next the aquifer is divided into 105 sub-domains, where each one covers approx. 4.5 × 4.5 km (l_x = l_y = 4.5 km) as shown in Fig. 3(b) and the overlapping zone is set equal to 1 km, hence between adjacent sub-domains there is a 2 km wide overlapping zone that is used to smooth the velocity. The solid black lines in Fig. 3(b) correspond to the sub-domain boundaries before the offset operator, while the grey lines represent the extended boundary. The constant head boundary conditions for the extended boundaries were interpolated from the coarse solution h^c. The sub-domains are simulated using the finite element approximation of the groundwater flow equation. For the fine solution we used 20 layers (vertical discretization) and a variable horizontal resolution. The elements size varies from a few metres near the wells to several tens of metres. Figure 3(c) shows the discretization of one of the sub-domains. The degrees of freedom (dof) for each subdomain vary since each sub-domain includes different geometric characteristics (wells, land use polygon). The total number of dof for the coarse approximation is 6.3×10^5, while for the fine resolution the dofs for each subdomain varies between 5.6×10^4 and 4.4×10^5 with an average of 2.6×10^5. Heads of the discretization nodes that lay within the overlapping zones are averaged according to the weighted scheme described previously.

The domain includes 1890 wells, therefore the NPSAT generates 189 000 URFs (100/well), which were stored into a GIS platform for use during the prediction phase.

Predictions

Loading functions are convoluted with the URFs, a computationally very inexpensive process. Flow and transport simulation time (construction phase) is on the order of several (~2) days,

however, the prediction phase for calculating the BTCs for 1890 wells is approx. 15 seconds. This negligible runtime allows the evaluation of multiple land use and NPS loading scenarios under different management and policy options and is also suited for optimization.

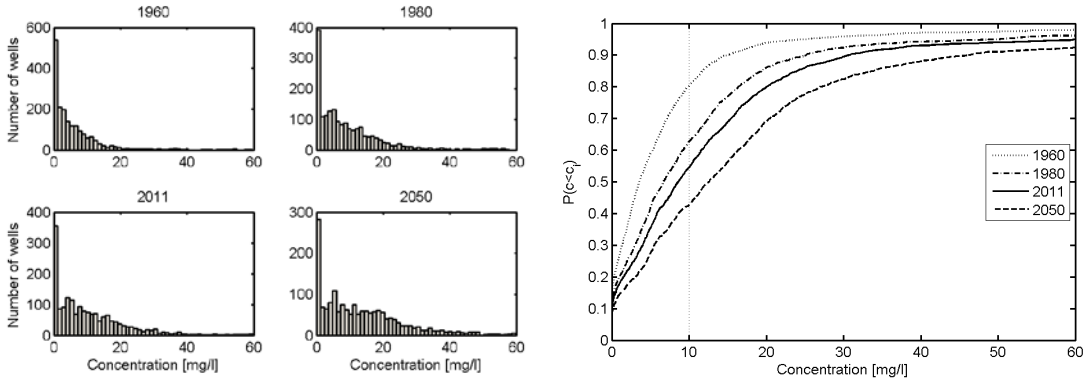

Fig. 4 Frequencies of the simulated nitrate occurrences (left), empirical cumulative distribution functions for the years 1960, 1980, 2011 and 2050 (right).

We present the frequencies of the simulated nitrate occurrences (left) for the years 1960, 1980, 2011, 2050 and the empirical cumulative distribution functions for the same years which express the probability of a well of not exceeding a certain value $P(c < c_i)$. Simulation results show that, in 1960, after 15 years of nitrate application at relatively low leaching rates (30–45% of current rates), 20% of wells exceed the nitrate (as N) drinking limit of 10 mg/L. Assuming that the leaching rates were linearly increased, approx. 37% of wells exceed the MCL in 1980 and 45% of the wells have concentrations above the MCL in 2011. Despite future reduction in nitrate leaching, the probability of wells exceeding the MCL increases to 58% by 2050. For 2006, a survey of domestic well nitrate (http://www.swrcb.ca.gov/gama/domestic_well.shtml#tularecfa) in Tulare County (approximately twice the area of, and including, the modelling area) found concentrations above the MCL for 40% of the sampled wells where the range of detection above the MCL varies between 10.1 and 54 mg/L. The distribution was skewed, similar to the prediction results. Deeper production wells generally have lower nitrate values than predicted.

CONCLUSIONS

We developed a computationally efficient approach to simulate regional nonpoint source pollution inputs to large-scale groundwater basins under conditions of spatio-temporally highly variable source loading to a widely distributed network of production wells. The approach provides the flexibility to simulate and evaluate multiple NPS loading scenarios and the potential for optimization of management practices. We use a two-step simplistic domain decomposition method to obtain a smooth, high resolution velocity field across very large simulation domains. Application to a large agricultural groundwater basin provides realistic estimates of current day nitrate distributions and suggests decadal to multi-decadal delay in NPS impacts to production wells of alluvial aquifer systems. The method needs to be further validated against time series data and for heterogeneous aquifer conditions.

Acknowledgements Funding was provided by the California State Water Resources Control Board Grant Agreement no. 04-184-555-0.

REFERENCES

Bower, H. (2000) Integrated water management: emerging issues and challenges. *Agric. Water Manage.* 45, 217–228.

Civita M., & De Maio, M. (2004) Assessing and mapping groundwater vulnerability to contamination: The Italian ‘‘combined’’ approach. *Geofisica Int* 43(4), 513–532.

Javadi, S., Kavehkar, N., Mousavizadeh, MH. & Mohammadi, K. (2011) Modification of DRASTIC model to map groundwater vulnerability to pollution using nitrate measurements in agricultural areas. *J. Agric. Sci. Technol.* 13(2), 239–249.

Kourakos, G., Klein, F, Cortis, A., & Harter, T. (2012) Groundwater non-point source pollution modeling using a 3D high resolution source-receptor unit response function approach. *Water Resour. Res.* (in print).

Nolan, B. T., Hitt, K. J. & Ruddy B. C. (2002) Probability of nitrate contamination in recently recharged groundwaters in the conterminous United States, *Environ. Sci. Technol*. 36(10), 2138–2145.

Ruud, N. C., Harter, T., Marques, G. F., Jenkins, M. W. & Lund, J. R. (2003) Modeling of Friant Water Management and Groundwater, Final Report, US Bureau of Reclamation, September 30, 2003, 294 pp.

Ruud, N., Harter, N. & Naugle, A. (2004) Estimation of groundwater pumping as closure to the water balance of a semi-arid, irrigated agricultural. *J. Hydrol*. 297(1–4), 51–73. doi: 10.1016/j.jhydrol.2004.04.014.

Sorichetta, A., Masetti, M., Ballabio, C., Sterlacchini, S. & Beretta, G. P. (2011) Reliability of groundwater vulnerability maps obtained through statistical methods. *J. Environ. Manage.* 92(4), 1215–1224, doi: 10.1016/j.jenvman.2010.12.009.

Watanabe, N., Bergamaschi, B. A., Loftin, K. A., Meyer M. T. & Harter, T. (2010), Use and environmental occurrence of antibiotics in freestall dairy farms with manure forage fields. *Environ. Sci. Technol.* 44(17), 6591–6600, doi: 10.1021/es100834s.

WWAP (World Wide Assessment Program) (2009) Water in changing world. *The United Nations World Water Development Report 3.*